Tunable Magnon Interactions in a Ferromagnetic Spin-1 Chain

Prashant Chauhan,[1] Fahad Mahmood,[1,*,‡] Hitesh J. Changlani,[2,3,1,†] S. M. Koohpayeh,[1] and N. P. Armitage[1]
[1]The Institute for Quantum Matter, Department of Physics and Astronomy, The Johns Hopkins University, Baltimore, Maryland 21218, USA
[2]Department of Physics, Florida State University, Tallahassee, Florida 32306, USA
[3]National High Magnetic Field Laboratory, Tallahassee, Florida 32304, USA

(Received 15 July 2019; revised manuscript received 7 October 2019; published 23 January 2020)

$NiNb_2O_6$ is an almost ideal realization of a 1D spin-1 ferromagnetic Heisenberg chain compound with weak unidirectional anisotropy. Using time-domain THz spectroscopy, we measure the low-energy electrodynamic response of $NiNb_2O_6$ as a function of temperature and external magnetic field. At low temperatures, we find a magnonlike spin excitation, which corresponds to the lowest energy excitation at $q \sim 0$. At higher temperatures, we unexpectedly observe a temperature-dependent renormalization of the spin-excitation energy, which has a strong dependence on field direction. Using theoretical arguments, exact diagonalizations, and finite temperature dynamical Lanczos calculations, we construct a picture of magnon-magnon interactions that naturally explains the observed renormalization. We show how magnetic field strength and direction may be used to directly tune the sign of the magnon-magnon interaction. This unique scenario is a consequence of the spin-1 nature and has no analog in the more widely studied spin-1/2 systems.

DOI: 10.1103/PhysRevLett.124.037203

Since the early work of Ising (1925) [1] and Bethe (1931) [2], magnetism in 1D spin chains has been the subject of continuous theoretical [3–13] and experimental interest [14–22]. Because of reduced dimensionality, magnetic order is susceptible to fluctuations that can cause the system to exhibit interesting quantum and classical effects [23]. Examples include novel quantum phase transitions [17,24], fractional excitations [25,26], entanglement [27], and spin-charge separation [28,29]. Moreover, the simplicity of 1D systems often makes the theoretical formulation tractable and allows a direct comparison with experiment.

Spin excitations in 1D chains have been studied for both ferromagnetic (FM) and antiferromagnetic (AFM) exchange interactions [4,15,18,30]. For an isolated FM spin-1/2 chain with dominant Ising interactions, the excitations are domain walls. Each spin flip forms two domain walls ("kinks" or "spinons") [31,32]. These fractional excitations can be understood analytically and have been studied extensively in a variety of 1D spin-1/2 systems [17–20].

The elementary excitation of a FM spin-1 chain is a magnonlike spin flip $|1\rangle \rightarrow |0\rangle$. This excitation has a well-defined energy and momentum and is relatively easy to understand. However, magnon-magnon interactions are possible leading to a renormalization of the spin excitation energies in ways that are quite distinct from the more commonly studied spin-1/2 chains. For example, as we will discuss below, in a spin-1 chain when two spin flips (two magnons) come together, they can tunnel into other configurations like $|00\rangle \rightarrow |1-1\rangle$ and $|-11\rangle$ to form a hybridized state which can alter the magnon spectrum. This process cannot occur in spin-1/2 chains.

The physics of such spin chains may be modeled with a nearest-neighbor exchange interaction J and an in-plane anisotropy strength D. For spin-1, weakly anisotropic chains $D < J$ with AFM interactions, one obtains the "Haldane gap," which has been the subject of extensive studies and is an early example of a symmetry protected topological phase [4]. For the FM case, one can obtain gapped or gapless excitations depending on the sign and size of D relative to J [8,9]. Little is understood about the FM case with $D < J$, unlike its AFM counterpart. There have been few theoretical studies (e.g., Refs. [8,33]), and even fewer experiments for this case.

Here we use time-domain THz spectroscopy (TDTS) to experimentally investigate the excitations of $NiNb_2O_6$ and their interactions. At low temperatures, we find spin excitations whose energies and magnetic field dependence correspond well to the single-magnon spectrum (at $q \sim 0$) of a 1D spin-1 Heisenberg ferromagnetic chain with weak unidirectional anisotropy. At higher temperatures, we observe a renormalization of the magnon energies that depends on the external field direction. This renormalization occurs due to magnon-magnon interactions that are a consequence of the spin-1 nature of the system and do not have an analog in the spin-1/2 chain. To address this, we employ the finite temperature dynamical Lanczos algorithm [34], and determine the effect of these interactions on the dynamical response at finite temperature. Our findings shed light on the unique nature of magnon interactions for a

spin-1 chain and give a general perspective on how TDTS in conjunction with numerical calculations can be used to understand finite temperature spin dynamics and interactions.

$NiNb_2O_6$ belongs to a family of quasi-1D compounds, the most prominent of which is the Co variant that is perhaps the best example we have of a quasi-1D spin-1/2 Ising system [17,18]. With Ni, the magnetism is both spin-1 and more isotropic. The structure consists [Fig. 1(a)] of zigzag edge-sharing chains of NiO_6 octahedra along the crystallographic c axis with ferromagnetic exchange interactions between nearest-neighbor spin-1 Ni^{+2} ions. Since the intrachain coupling along the c direction is significantly stronger than the interchain coupling ($J_{\parallel}/J_{\perp} \sim 20$) along the a or b direction, we can consider the system as an effective 1D spin-1 ferromagnetic chain with the c axis as its easy axis [35]. The spin Hamiltonian of this system in an external field can be described with Heisenberg exchange interactions with onsite anisotropy as follows:

$$H = -|J|\sum_{\langle i,j\rangle} \vec{S}_i \cdot \vec{S}_j - |D|\sum_i (S_i^z)^2 - g\mathbf{H}\cdot\sum_i \vec{S}_i, \quad (1)$$

where $-|J|$ is the ferromagnetic exchange interaction, D is the local onsite uniaxial anisotropy, S_i are spin-1 operators, and g is the coupling strength to the external field $\mathbf{H}$ (assuming an isotropic g tensor). Note that in our calculations, a, b, c refer to crystal directions, whereas x, y, and z correspond to spin quantization directions. Although an isolated chain with Ising anisotropy orders only at zero temperature, $NiNb_2O_6$'s FM chains order with AFM order below a temperature of 5.7 K due to weak interchain interactions. By fitting the specific heat and magnetization data Heid *et al.* [35] determined $J = 14.8$ K (0.308 THz), $D = 5.2$ K (0.11 THz), and $g = 2.3$.

The $NiNb_2O_6$ crystal was grown by the floating zone method and oriented by back reflection Laue diffraction (see Supplemental Material [36–40]). TDTS experiments were performed in external fields up to $\mathbf{H} = 68$ kG in both Faraday geometry with transverse field (wave vector $\mathbf{k}\|\mathbf{H}$, $\mathbf{H}\perp c$) and Voigt geometry with longitudinal field ($\mathbf{k}\perp\mathbf{H}$, $\mathbf{H}\|c$) at temperatures ranging from 4 to 150 K. The spectral range of our TDTS setup is limited to > 0.1 THz in the Faraday and > 0.15 THz in the Voigt geometries with a spectral resolution of $\sim$1 GHz. For magnetic insulators, TDTS functions as high-field electron spin resonance and allows a determination of the complex ac magnetic susceptibility $\tilde{\chi}(\nu) = \chi_1(\nu) + i\chi_2(\nu)$ at THz frequencies in the zero momentum limit. $\tilde{\chi}(\nu)$ is obtained after normalizing the transmission at a reference temperature (here 150 K) above the onset of magnetic correlations (see, e.g., Refs. [39,41–43]).

Figure 1(b) shows the magnitude of the transmission $T(\nu)$ of $NiNb_2O_6$ as a function of temperature down to 4 K with the THz wave-vector $\mathbf{k}\|a$ and the THz ac magnetic field $\mathbf{h}\|b$. In this orientation, a clear absorption peak is observed as the temperature is lowered. The low T peak center frequency of 0.11 THz at 4 K is in good agreement with anisotropy parameter $D = 0.11$ THz [35]. Note that in zero field, the local anisotropy term in D [Eq. (1)] breaks the isotropic symmetry of the Heisenberg term resulting in a gap of magnitude $|D|$ in the magnetic excitation spectrum as we observe [8]. To further understand these magnetic excitations, their dynamics and interactions in $NiNb_2O_6$, we perform TDTS measurements as a function of both magnetic field and temperature in both transverse and longitudinal geometries.

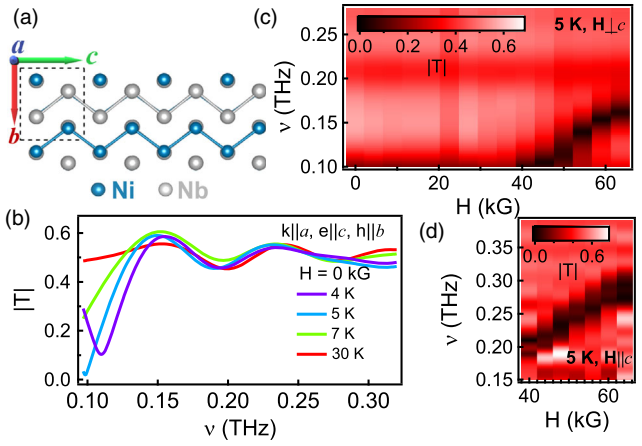

FIG. 1. (a) Ni spin-1 chains along the crystallographic c axis in the bc plane of $NiNb_2O_6$. (b) Transmission amplitude as a function of frequency ν in the absence of an external field ($H = 0$) for various temperatures. Here $\mathbf{k}\|a$, $\mathbf{e}\|c$, $\mathbf{h}\|b$, where $\mathbf{k}$ is the wave vector of the incident THz while $\mathbf{e}$ and $\mathbf{h}$ denote its ac electric and magnetic fields, respectively. (c)–(d) Field dependence of transmission at 5 K for both transverse and longitudinal field geometries, respectively.

Figures 1(c) and 1(d) show the field dependent transmission at 5 K in both transverse ($\mathbf{H}\perp c$) and longitudinal ($\mathbf{H}\|c$) field geometries. Magnon peaks are observed in both cases. The peak center frequency (ν_c) is extracted by fitting the imaginary part of complex magnetic susceptibility $\chi_2(\nu)$ to a Lorentzian [see Figs. 2(b) and 2(d)]. ν_c as a function of external magnetic field is shown in Fig. 2(a) for transverse geometry. At 5 K (dark blue squares), only the zero-field spectra and the spectra above 40 kG show excitations with $\nu_c > 0.1$ THz. Above 40 kG, ν_c varies linearly with field as $\nu_c \sim g\mu_B$ with an offset (μ_B is the Bohr magneton). From a linear fit to the data at 5 K (see Supplemental Material [36]), we extract a g factor of $g = 2.14$ which is in good agreement with Heid *et al.* [35]. The behavior of the magnon center frequency at 5 K is consistent with a field-induced ferromagnetic (FM) to paramagnetic (PM) phase transition in the spin-1 chain [35]. To understand the effect of thermal excitations on the magnetic spectra, we measure $\chi_2(\nu)$ at fixed field for various temperatures up to 110 K.

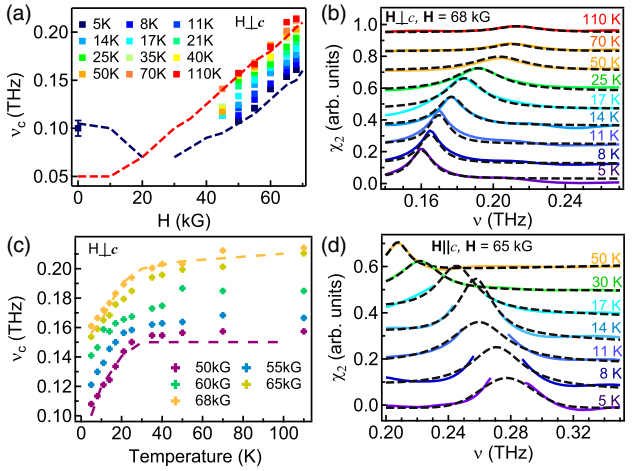

FIG. 2. (a) Field and (c) temperature dependence of the center frequency ν_c of the peak observed in χ_2 for $\mathbf{k}\|a$, $\mathbf{e}\|c$, $\mathbf{h}\|b$. Error bar in (a) represents a 95% confidence interval. Dashed lines are calculations as described in the text. (b) and (d) Imaginary part of the magnetic susceptibility $\chi_2(\nu)$ for various temperatures. $H = 68$ kG ($H\|a$) in (b) while $H = 65$ kG ($H\|c$) in (d). Dashed lines are fit to a Lorentzian. Note that the susceptibility data near the peak are unreliable in (d) due to very strong absorption. It was excluded from the plots and fits for this reason.

Figure 2(b) shows the temperature dependence of $\chi_2(\nu)$ at 68 kG in the transverse geometry. Clear magnon peaks are observed for temperatures up to 110 K. At each temperature, the measured magnon ν_c scales linearly with field for fields > 40 kG [Fig. 2(a)]. With increasing temperature, the peak height of the magnon reduces and the peak broadens as expected for thermal broadening of magnetic excitations. Interestingly, rather than staying constant, the magnon peak frequency shifts higher with increasing temperature for each field. In the absence of any transitions, this is quite unusual for magnetic excitations as they typically just broaden with increasing temperature and shift only slightly [18,39]. Figure 2(c) shows the temperature dependence of the magnon ν_c at different magnetic fields. ν_c increases linearly with temperature until ~30 K after which it asymptotically saturates. This agrees well with the temperature above which the susceptibility obeys the Curie-Weiss law (30 K [35]).

We carry out a similar analysis as described above in the longitudinal geometry ($\mathbf{H}\|c$) (see Supplemental Material [36]). Figure 2(d) shows the resulting $\chi_2(\nu)$ at 65 kG for various temperatures. In this orientation, we also observe magnetic excitations that weaken in intensity with increasing temperature. Importantly, the temperature dependence of the magnon peaks in the longitudinal geometry is *opposite* to that observed in the transverse geometry. Here, the magnon peaks shift towards *lower* frequencies with increasing temperature. Moreover, while there is some evidence for a field-induced phase transition in the transverse geometry (see Supplemental Material [36]), the behavior is different with the longitudinal field (see Supplemental Material [36]). Magnon center frequencies in both orientations show a linear dependence on the field at high fields with a similar g factors (see Supplemental Material [36]).

We posit that the field-dependent change in the magnon energies at higher temperature is indicative of magnon-magnon interactions renormalizing the excitation spectrum. To check this, we perform exact diagonalization (ED) calculations on the 1D Hamiltonian in Eq. (1) for chain length $L = 14$ at 0 K to determine the low-lying energy states of the system as a function of external field. Figures 3(a) and 3(b) show these excited state energies with respect to the ground state (GS) for transverse and longitudinal geometries, respectively, using the parameters $g = 2.14$, $J = 14.8$ K, and $D = 5.2$ K determined from earlier heat capacity and magnetization measurements [35]. Because a photon can only excite a single magnon with a spin change of $\Delta S = 1$, at 0 K only the first excited states ($E_{10} = E_1 - E_0$, where E_0 is the GS energy) are accessible with THz light [15]. These states are represented with bold points whose size represents the intensity of the excitations in TDTS experiments. These

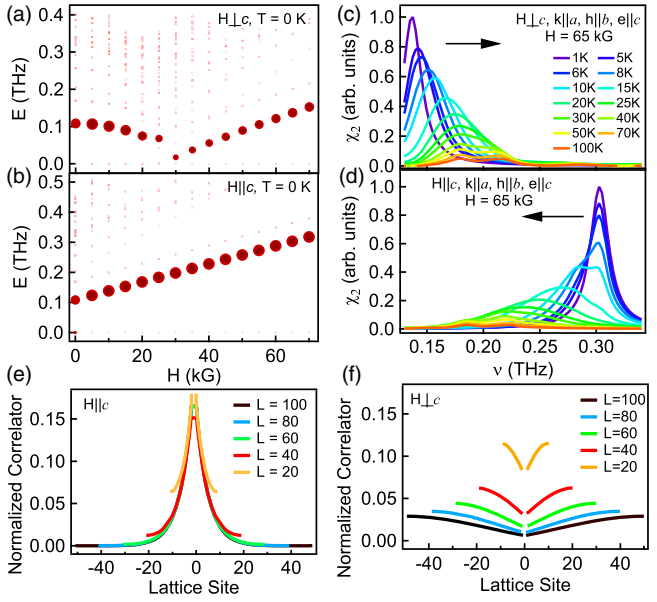

FIG. 3. Simulated excited state energy spectra (relative to the ground state) of the spin-1 chain ($L = 14$) as a function of external magnetic field (a) along the a axis and (b) the c axis. Bold points correspond to the excited states with the size of the big circles proportionate to $|\langle \text{Excited}|S^y|\text{Ground}\rangle|^2$. (c)–(d) Simulated temperature dependence of normalized χ_2 computed with finite temperature dynamical Lanczos at $H = 65$ kG in both transverse and longitudinal geometries with a Lorentzian used to broaden the spectra. The normalized magnon-magnon correlator (see text) for (e) transverse (assuming the two spin flip term can be ignored, see Supplemental Material [36]) and (f) longitudinal geometries with respect to a chosen reference site (labeled as site 0), evaluated in the lowest energy 2-magnon wave function in chains of different lengths, for $H = 70$ kG. The correlator of a site with itself has been omitted.

ED results match closely the measured excitation ν_c at 5 K for both transverse [Fig. 2(a)] and longitudinal geometries (see Supplemental Material [36]). In the transverse case, the ED results suggest a second order transition from the ferromagnetic to a paramagnetic phase, which is analogous to the phase transition in the spin-1/2 transverse field Ising model [15]. Since finite size effects near the critical point can be severe, additional DMRG calculations of the first two excited states were performed for a chain length of 200 to confirm this observation (see Supplemental Material [36]). For the longitudinal geometry [Fig. 3(b)], the ED calculations show no phase transition, as expected.

Having understood the field dependence of magnons in $NiNb_2O_6$ in the low temperature limit, we now turn to the principal unexpected finding in TDTS measurements, i.e., the unique temperature dependence of magnon energies—shift towards higher (lower) energies with increasing temperature in the transverse (longitudinal) geometries. In the low-temperature limit, it is only possible to excite one magnon due to an absorption of a photon, i.e., by making a transition from the GS to the first excited state (E_{10}). However, at higher temperatures ($T \gtrapprox E_{10}$), it becomes possible to have one-magnon transitions between higher energy states as well. At finite temperature, the one magnon states are thermally populated and a single photon absorption can also excite to two-magnon states with energy $E_{21} = E_2 - E_1$. In a harmonic model for the magnon spectrum (Holstein-Primakoff to quadratic order), all excited states should be equally spaced and as such, the excitation peak will always be centered at $\nu_c = E_{10} = E_{21}$ regardless of temperature. However, magnon-magnon interactions can renormalize the excitation spectrum resulting in energy shifts. To see how this arises in a spin-1 chain, we consider the effects of two-magnon interactions in both field geometries. For the longitudinal field, the energy of one magnon excitation ($|1\rangle \rightarrow |0\rangle$) is $E_{10} = 2SJ[1 - \cos(q)] + (2S-1)D + g\mu_B H$ [8], giving $E_{10} = D + g\mu_B H$ for $q = 0$ and $S = 1$, where the ground state ($\psi_{GS} = |1..111..1\rangle$) has energy $E_0 = -N(J + D + g\mu_B H)$. At zero field we get $E_{10} = D = 0.11$ THz which is exactly the energy of the first excited state observed at 5 K [Fig. 1(b)] in the TDTS measurements and in ED [Fig. 3(a)].

A two magnon state can be constructed by reducing the azimuthal spin by one unit at two different sites ($|..11111..\rangle \rightarrow |..1011011..\rangle$) giving an energy of $2E_{10}$ [8]. This is the case when the two magnons are well separated and not interacting with each other. However, when the two magnons are on adjacent sites, i.e., $|00\rangle$, then due to the spin-1 nature of the system the $|00\rangle$ configuration can tunnel into other spin-preserving states like $|00\rangle \rightarrow (|+1-1\rangle$ or $|-1+1\rangle)$, which can lower the total energy of the system. A crude approximation for the energy gained by the $|00\rangle$ magnons due to this hybridization is given by $E_{\text{gain}} = -(J + 2D/3)$, which gives $E_{21} = E_1 - E_0 - 2D/3 < E_{10}$ (See Supplemental Material [36]). This implies that there is an effective magnon *attractive* interaction creating a two-magnon bound state in longitudinal field. This attraction can also be verified from full diagonalization calculations on long chains up to $L = 100$ [44]—we find $E_{20} < 2E_{10}$ and from inspecting the spatial magnon-magnon correlator $L\langle(1-(S_z^i)^2)(1-(S_z^0)^2)\rangle$, with respect to the central site chosen to be "0"] for the energetically lowest 2-magnon wave function, shown in Fig. 3(e). Thus, with increasing temperature, we expect a shift of the effective excitation peak to lower frequencies as observed in longitudinal geometry [Fig. 2(d)]. Note that the process described cannot occur in the typically studied spin-1/2 case since two spin flips (or kinks) cannot tunnel into other spin-preserving configurations. In this regard spin-1 represents a special situation that is low spin enough to have strong quantum dynamics, but yet possess richer internal structure than spin-1/2.

In the transverse geometry when the external field H is large, the GS is nondegenerate and paramagnetic. For transverse field $H \gg D$, as is the case at 65 kG, the natural direction for spin quantization is along the a axis. In this case, the energy of the one magnon state is approximately $E_{10} = -(|D|/2) + g\mu_B H$ with $E_0 = -N(J + D/2 + g\mu_B H)$ (see Supplemental Material [36]). This reversal of sign in the D term at large transverse fields means that it costs energy to bring the two magnons adjacent to each other. This implies that there is an effective *repulsion* between two magnons in the transverse field paramagnetic phase, this is made more illuminating by observing the spatial magnon-magnon correlator in the energetically lowest 2-magnon wave function in Fig. 3(f) (see Supplemental Material [36]). Hence, with increasing temperature we have more repulsive interactions leading to a shift in the effective excitation peak to higher frequencies, which is as observed in the transverse geometry [Fig. 2(c)].

Within the models described above, we can qualitatively explain the observed shift in the magnon energies with temperature in terms of a renormalization of the spectrum based on effective magnon-magnon interactions. To further understand the observations, we calculate the finite temperature susceptibility using the finite temperature dynamical Lanczos algorithm [34] for a chain length $L = 14$. For $q = 0$, we calculate the frequency dependent correlation function as $C^{yy}(\nu, T) = (1/Z)\sum_{n,m} e^{-\beta E_n}|\langle m|S^y|n\rangle|^2\delta(E_n + \nu - E_m)$, where Z is the partition function, involving the sum over all eigenenergies, β is $1/k_B T$, E_n, and E_m are the energies of nth and mth eigenstates, respectively. At finite temperatures the excited states acquire finite lifetimes due to magnon decay processes. To compensate for the discrete spectra that arises from finite size effects, we broaden the delta functions using a Lorentzian description $\delta(\nu - \nu_{nm}) = \lim_{\epsilon\rightarrow 0}\{[\epsilon/\pi]/[(\nu - \nu_{nm})^2 + \epsilon^2]\}$, where $\nu_{nm} = E_m - E_n$ and a broadening $\epsilon = 0.01$ THz. We then calculate the dynamical susceptibility as $\chi^{yy}(\nu, T) = \pi(1 - e^{-\beta\nu})C^{yy}(\nu, T)$, which is equal to $\chi_2(\nu)$ [9].

Figures 3(c) and 3(d) show the simulated $\chi_2(\nu)$ at 65 kG at various temperatures for transverse and longitudinal geometries, respectively. In the transverse geometry, the magnon peaks in the calculated $\chi_2(\nu)$ shift towards higher frequencies with increasing temperature while the opposite is the case for the longitudinal geometry [Figs. 2(c) and 2(d)]. For a direct comparison between these calculations and the experiment, we plot the center frequencies of the peaks in the calculated $\chi_2(\nu)$ in the transverse geometry in Figs. 2(a) and 2(c) (dashed lines) at choice temperatures and fields. There is good agreement between the measured and calculated ν_c.

To conclude, we have provided experimental and theoretical evidence for magnon interactions in a ferromagnetic spin-1 chain through the observed shift in the peak frequencies with temperature in an external field. Depending on the field orientation, these interactions are either attractive or repulsive (at large transverse field). We note that while our experimental work relied on thermal excitations to generate and subsequently probe two magnons within linear response, one can imagine utilizing nonlinear THz spectroscopy with intense THz pulses to directly excite higher order states via two-photon absorption [45,46]. Subsequent interaction dynamics may be studied with the resulting nonlinear response of the system.

We thank O. Tchernyshyov for helpful conversations. Work at J. H. U. was supported through the Institute for Quantum Matter, an EFRC funded by the U.S. DOE, Office of BES under DE-SC0019331. H. J. C. thanks Florida State University and the National High Magnetic Field Laboratory for start up funds and XSEDE resources (DMR190020) and the Maryland Advanced Research Computing Center (MARCC) for computing time. The National High Magnetic Field Laboratory is supported by the National Science Foundation through NSF/DMR-1644779 and the state of Florida. The DMRG calculations in the Supplemental Material [36] were performed using the ITensor C++ library (version 2.1.1) [47].

*fahad@illinois.edu
†hchanglani@fsu.edu
‡Present address: Department of Physics, University of Illinois at Urbana-Champaign, Urbana, Illinois 61801-3080, USA

[1] E. Ising, Z. Phys. **31**, 253 (1925).
[2] H. Bethe, Z. Phys. **71**, 205 (1931).
[3] J. C. Bonner, H. W. J. Blöte, H. Beck, and G. Müller, in *Physics in One Dimension*, edited by J. Bernasconi and T. Schneider (Springer, Berlin, Heidelberg, 1981), pp. 115–128.
[4] F. D. M. Haldane, Phys. Rev. Lett. **50**, 1153 (1983).
[5] M. Weinert and A. Freeman, J. Magn. Magn. Mater. **38**, 23 (1983).
[6] I. Affleck, T. Kennedy, E. H. Lieb, and H. Tasaki, Commun. Math. Phys. **115**, 477 (1988).
[7] I. Affleck, J. Phys. Condens. Matter **1**, 3047 (1989).
[8] N. Papanicolaou and G. C. Psaltakis, Phys. Rev. B **35**, 342 (1987).
[9] N. Papanicolaou, A. Orendáčová, and M. Orendáč, Phys. Rev. B **56**, 8786 (1997).
[10] K. Damle and S. Sachdev, Phys. Rev. B **57**, 8307 (1998).
[11] T. Suzuki and S. I. Suga, Phys. Rev. B **98**, 180406(R) (2018).
[12] O. M. Sule, H. J. Changlani, I. Maruyama, and S. Ryu, Phys. Rev. B **92**, 075128 (2015).
[13] J. Richter, N. Casper, W. Brenig, and R. Steinigeweg, Phys. Rev. B **100**, 144423 (2019).
[14] M. Steiner, J. Villain, and C. Windsor, Adv. Phys. **25**, 87 (1976).
[15] K. Katsumata, J. Phys. Condens. Matter **12**, R589 (2000).
[16] S. Kimura, H. Yashiro, K. Okunishi, M. Hagiwara, Z. He, K. Kindo, T. Taniyama, and M. Itoh, Phys. Rev. Lett. **99**, 087602 (2007).
[17] R. Coldea, D. A. Tennant, E. M. Wheeler, E. Wawrzynska, D. Prabhakaran, M. Telling, K. Habicht, P. Smeibidl, and K. Kiefer, Science **327**, 177 (2010).
[18] C. M. Morris, R. Valdés Aguilar, A. Ghosh, S. M. Koohpayeh, J. Krizan, R. J. Cava, O. Tchernyshyov, T. M. McQueen, and N. P. Armitage, Phys. Rev. Lett. **112**, 137403 (2014).
[19] B. Grenier, S. Petit, V. Simonet, E. Canévet, L.-P. Regnault, S. Raymond, B. Canals, C. Berthier, and P. Lejay, Phys. Rev. Lett. **114**, 017201 (2015).
[20] Z. Wang, M. Schmidt, A. K. Bera, A. T. M. N. Islam, B. Lake, A. Loidl, and J. Deisenhofer, Phys. Rev. B **91**, 140404(R) (2015).
[21] Z. Wang, J. Wu, W. Yang, A. K. Bera, D. Kamenskyi, A. T. M. N. Islam, S. Xu, J. M. Law, B. Lake, C. Wu, and A. Loidl, Nature (London) **554**, 219 (2018).
[22] Q. Faure, S. Takayoshi, S. Petit, V. Simonet, S. Raymond, L.-P. Regnault, M. Boehm, J. S. White, M. Månsson, C. Rüegg, P. Lejay, B. Canals, T. Lorenz, S. C. Furuya, T. Giamarchi, and B. Grenier, Nat. Physics **14**, 716 (2018).
[23] N. D. Mermin and H. Wagner, Phys. Rev. Lett. **17**, 1133 (1966).
[24] S. Sachdev, *Quantum Phase Transitions* (Cambridge University Press, Cambridge, England, 2011).
[25] B. M. McCoy and T. T. Wu, Phys. Rev. D **18**, 1259 (1978).
[26] L. Faddeev and L. Takhtajan, Phys. Lett. A **85**, 375 (1981).
[27] N. Blanc, J. Trinh, L. Dong, X. Bai, A. A. Aczel, M. Mourigal, L. Balents, T. Siegrist, and A. P. Ramirez, Nat. Phys. **14**, 273 (2018).
[28] C. Kim, A. Y. Matsuura, Z.-X. Shen, N. Motoyama, H. Eisaki, S. Uchida, T. Tohyama, and S. Maekawa, Phys. Rev. Lett. **77**, 4054 (1996).
[29] A. Moreno, A. Muramatsu, and J. M. P. Carmelo, Phys. Rev. B **87**, 075101 (2013).
[30] D. Lissouck and J.-P. Nguenang, J. Phys. Condens. Matter **19**, 096202 (2007).
[31] S. B. Rutkevich, J. Stat. Phys. **131**, 917 (2008).
[32] P. Pfeuty, Ann. Phys. (N.Y.) **57**, 79 (1970).
[33] D. Spirin and Y. Fridman, J. Magn. Magn. Mater. **260**, 141 (2003).
[34] P. Prelovšek and J. Bonča, Ground state and finite temperature lanczos methods, in *Strongly Correlated Systems:*

Numerical Methods, edited by A. Avella and F. Mancini (Springer, Berlin, Heidelberg, 2013), pp. 1–30.
[35] C. Heid, H. Weitzel, F. Bourdarot, R. Calemczuk, T. Vogt, and H. Fuess, J. Phys. Condens. Matter **8**, 10609 (1996).
[36] See Supplemental Material at http://link.aps.org/supplemental/10.1103/PhysRevLett.124.037203 for details about the crystal growth and characterization, extracting $\tilde{\chi}(\nu)$ and temperature dependent dynamics calculations for both transverse and longitudinal fieldswhich include Refs. [37–40].
[37] H. Weitzel, Z. Kristallogr. **144**, 238 (1976).
[38] I. Yaeger, A. H. Morrish, and B. M. Wanklyn, Phys. Rev. B **15**, 1465 (1977).
[39] X. Zhang, F. Mahmood, M. Daum, Z. Dun, J. A. M. Paddison, N. J. Laurita, T. Hong, H. Zhou, N. P. Armitage, and M. Mourigal, Phys. Rev. X **8**, 031001 (2018).
[40] S. Giovanazzi, A. Görlitz, and T. Pfau, Phys. Rev. Lett. **89**, 130401 (2002).
[41] K. Kozuki, T. Nagashima, and M. Hangyo, Opt. Express **19**, 24950 (2011).
[42] L. Pan, S. K. Kim, A. Ghosh, C. M. Morris, K. A. Ross, E. Kermarrec, B. D. Gaulin, S. M. Koohpayeh, O. Tchernyshyov, and N. P. Armitage, Nat. Commun. **5**, 4970 (2014).
[43] N. Laurita, Low energy electrodynamics of quantum magnets, Ph.D. thesis, Johns Hopkins University, 2017.
[44] When only the 2-magnon sector is of interest, we have performed exact diagonalizations for chain lengths of up to 100 sites. See Supplemental Material [36] for more details.
[45] S. Takayoshi, Y. Murakami, and P. Werner, Phys. Rev. B **99**, 184303 (2019).
[46] Y. Wan and N. P. Armitage, Phys. Rev. Lett. **122**, 257401 (2019).
[47] M. Stoudenmire and S. R. White, www.itensor.org.